Available online at www.sciencedirect.com
ScienceDirect
Journal of Molecular Structure 837 (2007) 118–131
Journal of MOLECULAR STRUCTURE
www.elsevier.com/locate/molstruc

The generalized anomeric effect in the 1,3-thiazolidines: Evidence for both sulphur and nitrogen as electron donors. Crystal structures of various *N*-acylthiazolidines including mercury(II) complexes. Possible relevance to penicillin action

Sosale Chandrasekhar [a,*], Deepak Chopra [b], Kovuru Gopalaiah [a], Tayur N. Guru Row [b,*]

[a] *Department of Organic Chemistry, Indian Institute of Science, Bangalore 560 012, India*
[b] *Solid State and Structural Chemistry Unit, Indian Institute of Science, Bangalore 560 012, India*

Received 5 May 2006; received in revised form 2 October 2006; accepted 7 October 2006
Available online 13 December 2006

Abstract

Evidence for the generalized anomeric effect (GAE) in the *N*-acyl-1,3-thiazolidines, an important structural motif in the penicillins, was sought in the crystal structures of *N*-(4-nitrobenzoyl)-1,3-thiazolidine and its (2:1) complex with mercuric chloride, *N*-acetyl-2-phenyl-1,3-thiazolidine, and the (2:1) complex of *N*-benzoyl-1,3-thiazolidine with mercuric bromide. An inverse relationship was generally observed between the C_2–N and C_2–S bond lengths of the thiazolidine ring, supporting the existence of the GAE. (Maximal bond length changes were ~0.04 Å for C_2–N_3, S_1–C_2, and ~0.08 Å for N_3–C_6.) Comparison with *N*-acylpyrrolidines and tetrahydrothiophenes indicates that both the nitrogen-to-sulphur and sulphur-to-nitrogen GAE's operate simultaneously in the 1,3-thiazolidines, the former being dominant. (This is analogous to the normal and exo-anomeric effects in pyranoses, and also leads to an interesting application of Baldwin's rules.) The nitrogen-to-sulphur GAE is generally enhanced in the mercury(II) complexes (presumably *via* coordination at the sulphur); a 'competition' between the GAE and the amide resonance of the *N*-acyl moiety is apparent. There is evidence for a 'push–pull' charge transfer between the thiazolidine moieties in the mercury(II) complexes, and for a 'back-donation' of charge from the bromine atoms to the thiazolidine moieties in the $HgBr_2$ complex. (The sulphur atom appears to be sp^2 hybridised in the mercury(II) complexes, possibly for stereoelectronic reasons.) These results are apparently relevant to the mode of action of the penicillins.

Keywords: Amide resonance; Anomeric effect; Baldwin's rules; Crystal structure; β-Lactam; Mercury(II); Penicillin; Stereoelectronic; Thiazolidine; X-ray diffraction

1. Introduction

The 'generalized anomeric effect' (GAE) is a stereoelectronic term which refers to the preference for an antiperiplanar orientation of a carbon-heteroatom bond relative to an electron pair on another *geminally* situated heteroatom [1–3]. The possible existence of the GAE in the *N*-acyl-1,3-thiazolidines (**I**, Scheme 1) is interesting for both theoretical and practical reasons. Theoretically, because of the possibility of two opposing modes for the GAE: the sulphur as the donor with the nitrogen as the acceptor, or *vice versa*; and practically, because of the presence of the *N*-acyl-1,3-thiazolidine moiety in the penicillin antibiotics [4,5]. (The role of this moiety – if any – in penicillin action has not been clarified.)

The present structural study was thus undertaken in the hope that bond length changes would provide evidence for the sought after GAE – an approach that was very successful in pyranose systems [1]. There is also interesting precedent, crystal structures of well over a hundred

* Corresponding authors. Tel.: +91 80 2293 2689; fax: +91 80 2360 0529.
E-mail addresses: sosale@orgchem.iisc.ernet. in, ssctng@sscu.iisc.ernet.in (S. Chandrasekhar).

0022-2860/$ - see front matter © 2006 Elsevier B.V. All rights reserved.
doi:10.1016/j.molstruc.2006.10.034

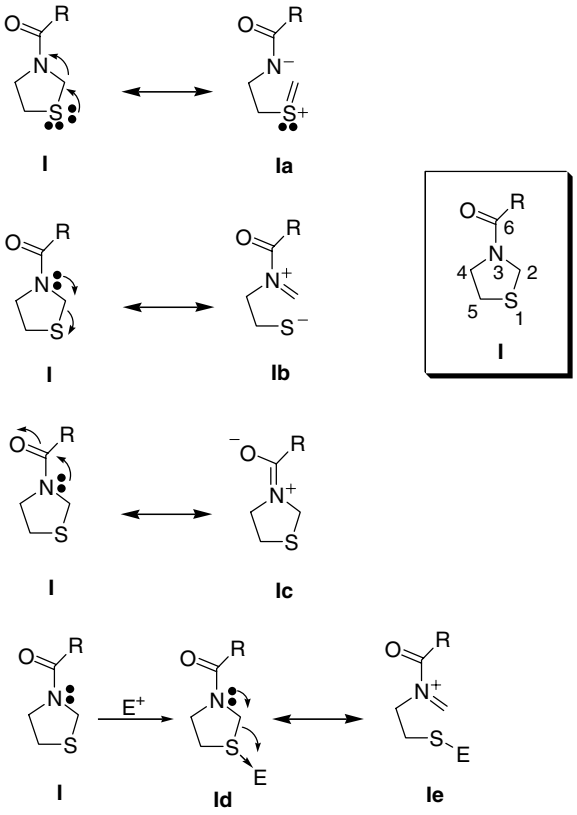

Scheme 1. The possible modes of the generalized anomeric effect (GAE) and competing charge transfers in *N*-acyl-1,3-thiazolidines **I**, represented by the canonical forms **Ia**–**Ie**: sulphur-to-nitrogen GAE (**Ia**), nitrogen-to-sulphur GAE (**Ib**), amide resonance (**Ic**), attack of electrophile ('E') at sulphur (**Id** and **Ie**). The boxed structure shows the numbering scheme employed for **I.**

1,3-thiazolidine derivatives having been reported (although no *N*-acyl derivatives, apparently). A random sampling of these reports [6–8] indicates a general inverse relationship between the *C–N* and *C–S* bond lengths of the thiazolidine moiety (although with exceptions, cf. Table 1). This is significant as analogous trends in the pyranoses have been considered to evidence the anomeric effect [1]. Of particular interest in the present study was the effect of the *N*-acyl moiety on these trends.

Simple, readily prepared and crystalline *N*-acyl-1,3-thiazolidine analogs were thus sought and subjected to X-ray diffraction analysis. Four analogs were so studied (**1**–**4**, Scheme 2), two being mercury(II) complexes (**3** and **4**) as these were expected to indicate how electrophilic coordination at the sulphur atom would modulate the GAE.

Table 1
Typical values of the relevant anomeric bond lengths (in Å) in substituted 1,3-thiazolidine derivatives possibly evidencing the GAE[a]

Derivative	C_2–N_3	S_1–C_2
Tricyclic penam[b]	1.474 (5)	1.810 (4)
4-Carboxylic acid[c]	1.463 (7)	1.852 (8)
Octahydrobenzothiazole[b]	1.441 (4)	1.868 (3)
4-Carboxylic acid[c]	1.484 (7)	1.869 (6)
2-Phenyl[d]	1.454 (2)	1.882 (2)

[a] From a random sampling of reported crystal structure data (standard deviations in parenthesis).
[b] Ref. [6].
[c] Ref. [7].
[d] Ref. [8].

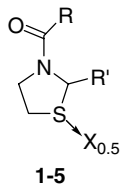

1-5	X	R'	R
1	-	H	*p*-(NO_2)-C_6H_5-
2	-	Ph	Me
3	$HgCl_2$	H	*p*-(NO_2)-C_6H_5-
4	$HgBr_2$	H	Ph
5	-	H	Ph

Scheme 2. *N*-Acyl-1,3-thiazolidine derivatives prepared and studied in this work, *via* X-ray diffraction determination of the crystal structures (except **5**). The indicated stoichiometry of 0.5 for 'X' above implies that two molecules of the thiazolidine bind to one of the mercuric halide in the case of **3** and **4** (cf. Schemes 4 and 5 below for the full structures).

In the *N*-acyl-1,3-thiazolidines the GAE would act alongside the amide resonance of the *N*-acyl moiety: either in concert (sulphur as donor) or in opposition (nitrogen as donor). These two GAE modes may be conveniently represented by the no-bond canonical forms **Ia** and **Ib**, respectively, **Ic** then representing amide resonance (cf. Scheme 1). The above two modes may be termed the 'sulphur-to-nitrogen' and 'nitrogen-to-sulphur' GAE's, respectively. The anomeric effect (~2 kcals/mole) [1–3] is, of course, much weaker than amide resonance (~20 kcals/mole) [9]; however, it is conceivable that electrophilic coordination at the sulphur centre would enhance the 'nitrogen-to-sulphur' GAE in **I** (cf. **Id** and **Ie**), thereby opposing and weakening the amide resonance.

Other interesting questions pertain to whether or not the amide nitrogen atom in **I** would be pyramidalised by the nitrogen-to-sulphur GAE, and to the conformation of the thiazolidine ring. In fact, the above modes of charge transfer could possibly be of importance in the mode of action of the penicillins [5], as will be discussed later.

The principles of stereoelectronic theory, particularly as apply to the 'antiperiplanar lone pair hypothesis' (ALPH) have been the subject of numerous reviews [1–3], and will not be elaborated upon herein. A basic familiarity with these principles is assumed in this paper, particularly the idea of the overlap of electron lone pairs with adjacent and suitably aligned antibonding (σ^*) orbitals. (Thus, in the nitrogen-to-sulphur GAE the lone pair of electrons on the nitrogen atom would overlap with the C_2–S σ^* orbital; in the sulphur-to-nitrogen GAE a lone pair on the sulphur atom would overlap with the C_2–N σ^* orbital.)

2. Experimental

2.1. General remarks

Organic compounds were prepared and characterized with the following instruments: JASCO FT/IR 410 IR

Spectrometer, JEOL JNM-LA 300 FT NMR System (^{1}H at 300 MHz and ^{13}C at 75 MHz), Micromass Q-TOF AMPS MAX 10/6A Mass spectrometer. NMR spectra were recorded in $CDCl_3$ solution with tetramethylsilane as internal standard (unless stated otherwise), and IR spectra as stated. The X-ray diffraction studies are described separately below.

1,3-Thiazolidine and its 2-phenyl derivative were prepared from 2-aminoethanethiol and the appropriate aldehyde by reported procedures [10,11], and *N*-acylated to obtain **1**, **2** and **5** as described below [12] (cf. Scheme 2); these were converted to their mercury(II) complexes **3** and **5**, respectively, [13]. Interestingly, all these amide derivatives exhibited hindered rotation around the amide *C–N* double bond and gave rise to twin resonances in the NMR. (These were generally broad multiplets, 'br m', as indicated below in the NMR data; note that the total integration value of the twin peaks is given.) Variable temperature NMR studies in two cases (**1** and **5**) were also performed as described further below.

2.2. Preparation of the N-acyl-1,3-thiazolidines (general procedure)

A stirred solution of the thiazolidine (5.0 mmol) in dry CH_2Cl_2 (6.0 ml), at 0 °C and under nitrogen, was treated with a solution of the acid chloride (or the anhydride) (5.2 mmol) in dry CH_2Cl_2 (6.0 ml) over 0.25 h. The reaction mixture was maintained at 0 °C for an additional 0.5 h and allowed to warm to 25°C. The mixture was then worked up by diluting with CH_2Cl_2 and washing with saturated $NaHCO_3$ solution (10 ml) and water (2 × 20 ml). The organics were dried (Na_2SO_4) and distilled *in vacuo* to remove solvent. The resulting crude residue was purified by column chromatography over silica gel to obtain the pure product.

Thus, *N*-(4-nitrobenzoyl)-1,3-thiazolidine (**1**) was obtained from thiazolidine and 4-nitrobenzoyl chloride in 92% yield as a pale yellow solid; mp 71–74 °C; ν_{max} (cm^{-1}) ($CHCl_3$) 1637, 1599, 1521, 1418; δ_H 3.05 and 3.14 (2H, 2× br m, C_5–H), 3.75 and 4.02 (2H, 2× br m, C_4–H), 4.47 and 4.77 (2H, 2× br m, C_2–H), 7.73 (2H, d, $J = 8.4$ Hz, Ar-H *ortho* to C=O), 8.29 (2H, d, $J = 8.4$ Hz, Ar-H *ortho* to NO_2); δ_C 29.5 and 30.8 (C_5), 48.0 and 48.2 (C_4), 50.7 and 51.3 (C_2), 123.4 (C_{aryl} *ortho* to C=O), 127.9 (C_{aryl} *ortho* to NO_2), 141.6 and 142.0 (C_{aryl} at C=O in the two amide rotamers), 148.3 (C_{aryl} at NO_2), 166.8 (*C*=O); *m/e* 238 (M^+), 210, 150 (100%), 104; HRMS: calcd. for $C_{10}H_{10}N_2O_3SNa$ (M + Na) 261.0310 (Found 261.0315).

N-Acetyl-2-phenyl-1,3-thiazolidine (**2**) was obtained from 2-phenylthiazolidine and acetic anhydride in 89% yield as a colourless solid; mp 65–68 °C (reported [11] 64.3–64.8 °C); ν_{max}/cm^{-1} ($CHCl_3$) 1650, 1401, 1352, 726; δ_H 1.96 and 2.19 (3H, 2 × s, –CO-*Me*), 3.04–3.17 (2H, m, C_5–H), 3.90–3.99 and 4.25–4.31 (2H, 2 × m, C_4–H), 6.01 and 6.50 (1H, 2 × s, C_2–H), 7.22–7.39 (5H, m, Ar-H); δ_C 22.7 and 23.1 (CO-*Me*), 28.9 and 30.4 (C_5), 50.2 and 50.7 (C_4), 64.0 and 65.0 (C_2), 125.1 and 125.7 (phenyl C_4), 127.5 and 128.0 (phenyl C_2, C_6), 128.3 and 128.8 (phenyl C_3, C_5), 141.4 and 141.7 (phenyl C_1), 168.3 and 169.1 (*C*=O); *m/e* 207 (M^+), 179 (100%), 164, 118; HRMS: calcd. for $C_{11}H_{13}NOSNa$ (M + Na) 230.0616 (Found 230.0621).

N-Benzoyl-1,3-thiazolidine (**5**) was obtained from the thiazolidine and benzoyl chloride in 95% yield as a colorless liquid. ν_{max}/cm^{-1} (thin film)1634, 1576, 1402; δ_H 3.01 (2H, br m, C_5–H), 3.75 and 3.96 (2H, 2 × br m, C_4–H), 4.49 and 4.73 (2H, 2 × br m, C_2–H), 7.33–7.51 (5H, m, Ar-H); δ_C 30.4 (C_5), 48.0 (C_4), 51.3 (C_2), 126.9 (phenyl C_2, C_6), 128.1 (phenyl C_3, C_5), 130.1 (phenyl C_4), 135.9 (phenyl C_1), 169.3 (*C*=O); *m/e* 193 (M^+), 165, 105, 83 (100%); HRMS: calcd. for $C_{10}H_{11}NOSNa$ (M + Na) 216.0459 (Found 216.0463).

2.3. Preparation of the mercury(II) complexes 3 and 4

These were prepared from **1** and **5** by a modification of a reported procedure [13]. Thus, a stirred solution of the nitrobenzoylthiazolidine **1** (3.0 mmol) in ethanol (15 ml) was treated with a warm ethanolic solution of $HgCl_2$ (0.2 *M*, 15 ml), when a white precipitate resulted. The mixture was allowed to cool and filtered to collect the precipitate, which was washed with ethanol and dried (Na_2SO_4) *in vacuo*. The solid was recrystallised from acetone to obtain the pure complex **3** as colourless crystals (2.0 mmol, 66%); mp 110–114 °C; ν_{max}/cm^{-1} (KBr) 1650, 1634, 1596, 1514, 1416, 1345, 844; δ_H (acetone-d_6) 2.93 and 3.12 (2H, 2 × br m, C_5–H), 3.81 and 3.93 (2H, 2 × br m, C_4–H), 4.59 and 4.72 (2H, 2 × br m, C_2–H), 7.85 (2H, d, $J = 8.4$ Hz, Ar-H *ortho* to C=O), 8.34 (2H, d, $J = 8.4$ Hz, Ar-H *ortho* to NO_2); δ_C 48.5 and 49.2 (C_5), 51.3 and 51.4 (C_4), 52.1 and 52.2 (C_2), 124.4 (C_{aryl} *ortho* to C=O), 129.4 (C_{aryl} *ortho* to NO_2), 143.7 (C_{aryl} at C=O), 149.5 (C_{aryl} at NO_2), 167.7 (*C*=O).

The mercuric bromide complex **4** was similarly prepared from *N*-benzoylthiazolidine (**5**) and mercuric bromide as a colourless crystalline solid in 59% yield; mp 140–143 °C; ν_{max}/cm^{-1} (KBr) 1626, 1575, 1393; δ_H (acetone-d_6) 2.91 and 3.08 (2H, 2 × br m, C_5–H), 3.86 (2H, br m, C_4–H), 4.64 (2H, br m, C_2–H), 7.46–7.58 (5H, m, Ar-H); δ_C 45.7 and 47.2 (C_5), 51.28 and 51.32 (C_4), 57.0 and 57.5 (C_2), 128.2 (C_{aryl} *ortho* to C=O), 129.1 (C_{aryl} *ortho* to NO_2), 131.0 (C_{aryl} at C=O), 137.5 (C_{aryl} at NO_2), 169.8 (*C*=O).

2.4. Variable temperature NMR studies of 1 and 5: hindered rotation around the amide bond [9]

The *N*-acylthiazolidines **1**–**5** exhibited hindered rotation around the amide *C–N* bond in the NMR, a pair of signals being seen for a particular proton or carbon atom in most cases as indicated above. Variable temperature ^{1}H NMR studies were performed in the case of the nitrobenzoyl derivative **1** and the benzoyl derivative **5**, and these showed that the twin resonances for each proton of the thiazolidine

ring were considerably broadened in both cases, but much more so in the case of **5**, at room temperature. Furthermore, at +50 °C the resonances were sharper in the case of **5** than in the case of **1**. These apparently indicate that the interconversion of the amide rotamers in **1** is slower than in **5**. Thus, the partial double bond of the amide *C–N* moiety has greater double bond character in **1** than in **5**, presumably a consequence of the greater electron withdrawing ability of the 4-nitrophenyl group relative to a phenyl group. (Both **1** and **5** exhibited very sharp resonances at −78 °C, indicating that interconversion of the amide rotamers has almost completely ceased.)

2.5. X-ray diffraction studies

Single crystal X-ray diffraction studies of the *N*-acylthiazolidine derivatives **1–4** prepared and characterized as above, were performed on a Bruker AXS SMART APEX CCD diffractometer using graphite monochromatic Mo Kα radiation. The data was collected at room temperature using an Oxford N_2 cryosystem. The data was collected using the package SMART and the data reduction was carried out using SAINTPLUS. An empirical absorption correction was performed with SADABS. Reduced intensities were analyzed using XPREP for the space group determination and merging. All the structures were solved using SIR92 and refined using SHELXL present in the WinGx (Version 1.64.05) program suite. All the hydrogen atoms for these structures were located from the difference Fourier map and refined accordingly. ORTEP diagrams of all the compounds were generated by ORTEP32. The geometric calculations were done by PARST95. Full details of these studies, including the relevant references, have been deposited in the Cambridge Crystallographic Database [14].

The relevant crystallographic data of **1–4** have been collected and tabulated in the 'Appendix' section, along with a brief note on the lattice packing characteristics.

3. Results and discussion

3.1. Crystal structures of the N-acyl-1,3-thiazolidines 1–4: general trends

Crystalline **1–4** were prepared and studied by X-ray diffraction [14] as described above. The relevant bond length data are summarized in Table 2. Two important trends are noteworthy. Firstly, both the endocyclic C_2–S and C_2–N bonds are shortened relative to the corresponding carbon-heteroatom bonds in tetrahydrothiophene [15] and pyrrolidine [16], respectively (cf. Table 3). Secondly, there is a general inverse relationship between the endocyclic C_2–S and C_2–N lengths, as also between the endocyclic C_2–N and exocyclic C_6–N lengths. Intriguingly, the $C{=}O$ bond lengths are only marginally affected.

These trends are not without exception, although plots of the data in Table 2 afford approximate linear fits if one of the points is excluded in most cases (cf. Figs. 5–8 in the 'Appendix'.) The maximal bond length changes in **1–4** are ~0.04 Å for C_2–N_3 and S_1–C_2, >0.08 Å for N_3–C_6 and ~0.017 Å for $C_6{=}O$ (cf. Table 2).

Table 2
Relevant bond distances (in Å) in the 1,3-thiazolidine derivatives **1–4** determined by X-ray diffraction in this study[a]

Compound	N_3–C_6	$C_6{=}O$	C_2–N_3	C_2–S_1
1	1.337(8)	1.223(7)	1.477(8)	1.785(8)
2	1.354(3)	1.224(3)	1.458(3)	1.832(2)
3a	1.359(4)	1.223(4)	1.437(5)	1.832(5)
3b	1.349(4)	1.228(4)	1.468(4)	1.807(4)
4a	1.355(1)	1.218(2)	1.441(2)	1.787(3)
4b	1.277(2)	1.239(2)	1.460(2)	1.793(3)

[a] The 2:1 mercury(II) complexes **3** and **4** provide two separate sets of data for the two different thiazolidine moieties (indicated by '**a**' and '**b**', cf. Schemes 2, 4 and 5); standard deviations are given in parenthesis.

Table 3
Typical carbon-heteroatom bond distances (in Å) reported for crystalline derivatives of tetrahydrothiophene (*C–S*) and *N*-acylpyrrolidine (*C–N* and *N–CO*), as determined by X-ray diffraction

Compound	*C–S*	*C–N*	*N–CO*
Tetrahydrothiophene[a]	1.84	–	
N-Acylpyrrolidine[b]	–	1.49	1.35

[a] Ref. [15].
[b] Ref. [16].

The site of complexation in the mercuric complexes **3** and **4** is the sulphur atom in both the cases studied (as expected). Both **3** and **4** were composed of two molecules of thiazolidine and one of mercury halide. Also, **3** was dimeric and pentacoordinated, whereas **4** was monomeric and tetracoordinated, at the mercury atom. (The difference in coordination numbers is possibly due to the greater electrophilicity of mercuric chloride relative to mercuric bromide.)

In general – although not invariably – the complexes **3** and **4** apparently evidence an increase in the nitrogen-to-sulphur GAE relative to **1** and **2.** Furthermore, both **3** and **4** furnish differing sets of data for the two thiazolidine ligands in each of them (denoted as '**a**' and '**b**'). Accordingly, the effect of the complexation on the structural features of the thiazolidine ring are complicated in an interesting manner.

The amide resonance of the N_3-acyl moiety apparently increases with increasing electron withdrawal at the acyl carbonyl atom (C_6), as indicated by the N_3–C_6 distance. This length is expected to be inversely related to the extent of amide resonance, and is thus at (nearly) a minimum in the *p*-nitrophenyl derivative **3**. (An exception is the mercuric bromide complex **4**, as discussed further below.)

There is no discernible pyramidalisation of the ring nitrogen atom in any of the derivatives studied; however, the thiazolidine ring is puckered although not uniformly. (The annular bond angles at the heteroatoms are apparently normal and generally show little variation.)

Another interesting trend is that almost all the derivatives **1**–**4** crystallise with the amide $C_6{=}O$ bond in the antiperiplanar orientation relative to the endocyclic C_2–N bond (with only one exception).

The above trends and structural features are discussed in detail below.

3.2. Relative shortening of the (endocyclic) S_1–C_2 and C_2–N bonds: competing 5-endo-trig processes

Crystallographic studies on numerous derivatives of both tetrahydrothiophene [15] and *N*-acylpyrrolidine [16] have been reported, and typical carbon-heteroatom bond lengths are collected in Table 3. Thus, the *C*–*S* lengths are generally >1.80 Å, and the *C*–*N* lengths generally >1.47 Å. These compare interestingly with the values determined in this study for **1**–**4** (Table 2). Thus, the S_1–C_2 length in the thiazolidines can be as low as 1.7849 Å, and the C_2–N_3 length as low as 1.4371 Å. (Note that electron-withdrawal by the *N*-acyl moieties in **1**–**4** would mute the nitrogen-to-sulphur GAE, so the above changes should be greater in principle.)

A possible explanation for these trends is the simultaneous operation of both the modes of the GAE, *i.e.*, involving both the nitrogen and the sulphur centres as donors (cf. Scheme 1). (A similar effect is the operation of both *exo* and *endo* anomeric effects in the pyranose sugars [1,2]). The extent of the bond shortening in **1**–**4** indicates that the anomeric interaction involving the nitrogen centre as the donor is the stronger one [17]. This is intriguing not only because sulphur is regarded as a better donor than nitrogen [2,18], but also because the nitrogen centre bears an electron-withdrawing acyl group.

However, this could be related to the fact that 1,3-thiazolidines undergo ring-opening *via* cleavage of the C_2–S bond (Eq. (1), Scheme 3) rather than of the C_2–N bond (Eq. (2), Scheme 3) [4,19]. This is explicable on the basis of Baldwin's rules [20]: Eq. (1) represents a favoured 5-*endo*-trig process involving a second row element (sulphur), but Eq. (2) a disfavoured 5-*endo*-trig process involving a first row element (nitrogen). These arguments imply that of the two no-bond canonical forms **Ia** and **Ib**, the former would be higher in energy, and would thus contribute less towards the overall charge transfer in the molecule.

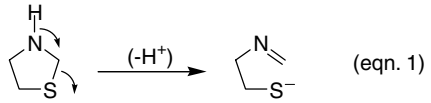

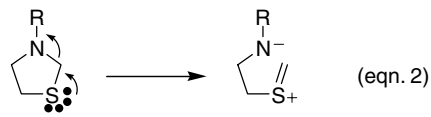

Scheme 3. Two possible modes for the ring opening of 1,3-thiazolidine: both are 5-*endo*-trig processes, but Eq. (1) is favoured over Eq. (2).

In fact, the rather low pK_a of 6.3 reported for 1,3-thiazolidine [21] indicates a relatively stabilized conjugate base form, possibly due to electron withdrawal by the sulphur atom *via* the nitrogen-to-sulphur GAE. (The magnitude of the pK_a apparently rules out a simple inductive effect).

3.3. Inverse relationship between C–S and C–N lengths

In principle, an observed inverse relationship between the C_2–S and C_2–N lengths may arise from either of the two modes of the GAE, involving either the sulphur or the nitrogen as the donor centre. However, in the light of the above discussion the latter mode is presumably the dominant one.

The best inverse correlation is apparently that between the endocyclic C_2–N and exocyclic N_3–C_6 lengths, the only exception being an unusually short exocyclic value of 1.2768 Å in **4b** (Table 2). The correlation between the endocyclic C_2–N and C_2–S lengths is beset with several exceptions, although these may well arise from the disparate substitution pattern in the overall molecule. Thus the correlation between the uncomplexed **1** and **2** is good, with a decrease in the endocyclic C_2–N length being accompanied by an increase in the endocyclic C_2–S length on going from **1** to **2.** This (expectedly) follows a decrease in electron withdrawal at the amide carbonyl group, the substituent therein changing from *p*-nitrophenyl to methyl. Although the role of the C_2 phenyl substituent in **2** is unclear, the overall trend indicates an enhanced nitrogen-to-sulphur GAE (in **2** relative to **1**).

Another good correlation is that between the *p*-nitrobenzoyl derivative **1** and its mercuric chloride complex **3**. The shortening of the endocyclic C_2–N length and the corresponding lengthening of the C_2–S in **3**, indicate an enhanced nitrogen-to-sulphur GAE, most likely due to electrophilic coordination by mercury(II) at the sulphur atom (in both **3a** and **3b**).

Both the above two cases involving the pairs **1/2** and **1/3**, demonstrate electronic effects at the termini of the *N*–*C*–*S* system in 1,3-thiazolidine. These are also accompanied by corresponding changes in the exocyclic amide N_3–C_6 lengths, which correlate inversely with the endocyclic C_2–N lengths and directly with the C_2–S lengths. This clearly establishes a 'competition' between amide resonance and the GAE, the electron pair at the nitrogen centre being effectively partitioned between the amide and *C*–*N*–*S* systems. [Similar trends are discernible in 2-phenyl-1,3-thiazolidine (cf. Table 1) [8] and its *N*-acetyl derivative **2** (this study, cf. Table 2).]

3.4. The Hg(II) complexes: the 'push–pull' mechanism in 3 and 4

The data of the two mercury(II) complexes **3** and **4** (each involving two thiazolidine units) show two interesting trends, discussed below. (Tetrahydrothiophene reportedly reacts with mercuric chloride *via* nucleophilic displacement

of a chloride ion rather than forming a complex [22]; this indicates that tetrahydrothiophene is more nucleophilic than **1** and possibly **5**, presumably because of the electronegative *N*-acyl moiety in **1** and **5**.)

The first trend is that in the mercuric chloride complex **3** the endocyclic C_2–*N* and C_2–*S* lengths in the two thiazolidine moieties correlate inversely (cf. Table 2), as do the endocyclic C_2–*N* and exocyclic C_6–*N* lengths. Clearly, the above arguments proposed for the pairs **1/2** and **1/3** apply here too.

Interestingly, the inverse trends in **3** apparently imply a 'push–pull' mechanism, in which charge is transferred from one thiazolidine ligand through the mercury atom to the other thiazolidine ligand (cf. the no-bond form **IV** in Scheme 4). This indicates that the nitrogen-to-sulphur GAE dominates in thiazolidine ligand **3a**, and the sulphur-to-nitrogen GAE in ligand **3b** (Scheme 4). There are also corresponding changes in the *N*-acyl moieties (amide resonance is enhanced in **3b** relative to **3a**).

Similar trends also exist in the mercuric bromide complex **4** (although with an interesting exception). Thus, in the two thiazolidine moieties **4a** and **4b**, the exocyclic C_6–*N* length is inversely related to both the C_6=*O* and C_2–N_3 lengths. Intriguingly, however, these changes are not matched by the C_2–*S* lengths, which relate directly with the C_2–*N* lengths. This indicates an enhanced GAE in both the modes in **4a**, which is discussed in the next section. Also, the minimal N_3–C_6 length (1.2768 Å) and the matching maximal C_6=*O* length (1.2390 Å) in **4b** evidence the maximum level of amide resonance in this set of derivatives.

The second trend (mentioned above) is the increase in the endocyclic C_2–N_3 length (Table 2) on going from the mercuric chloride complex **3** to the mercuric bromide complex **4**, although this is only relative to **3a**; the exocyclic amide C_6–*N* length is drastically shortened (1.2768 Å as mentioned) in **4b;** the C_2–*S* length is also inversely related to the C_2–*N* length in this set (*i.e.*, **3a** *vs.* either **4a** or **4b**). The likely explanation is that the lower electrophilicity of mercuric bromide decreases the nitrogen-to-sulphur GAE relatively in **4a** and **4b**. (The bond distances also indicate that the 'push–pull' effect is greater in **3** than in **4**.)

The trends involving C_2–N_3 vanish if **3b** is compared with **4a** or **4b**, possibly because **3b** possesses an unusually low nitrogen-to-sulphur GAE, and an enhanced sulphur-to-nitrogen GAE (because of the 'push–pull' effect). These seem to overcome the difference in electrophilicity mentioned above.

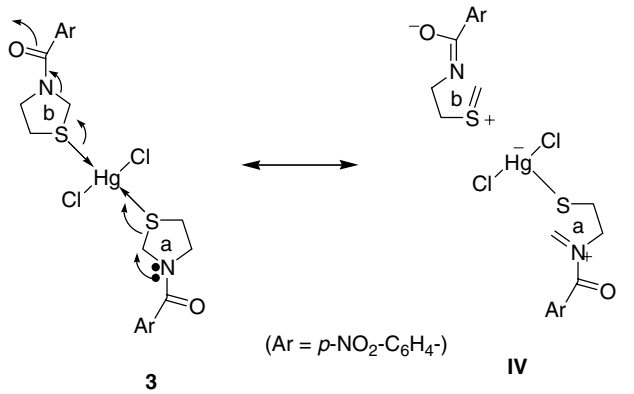

Scheme 4. The 'push–pull' mechanism for charge transfer in the $HgCl_2$ complex **3**, in which the nitrogen-to-sulphur GAE operates in one ring (marked 'a') and the sulphur-to-nitrogen GAE in the other (marked 'b'). (These correspond with **3a** and **3b**, respectively in Tables 2,5,6,8 and 9.)

3.5. The Hg(II) complexes: the 'back-donation' mechanism in 4

Not only does the C_2–*N* distance decrease on going from **3b** to **4a** or **4b**, but so too does the C_2–*S* distance! A similar trend involves **4a** and **4b** (but N_3–C_6, C_6=*O* and C_2–N_3 behaving as expected).

These trends apparently imply an enhanced GAE in both the modes, *i.e.*, with both the nitrogen and sulphur centres acting as donors, and which increases in the series **3b**–**4b**–**4a**. A possible explanation for this could be that there is a back-donation of electrons from the sulphur atom to the C_2 centre, which progressively increases in the above series.

Considering first the set **4a** and **4b**, such a back donation would overlay an enhanced sulphur-to-nitrogen GAE on the nitrogen-to-sulphur GAE in ring **4a** (cf. no-bond forms **V** and **VI**, Scheme 5). It is possible that an electron lone pair is donated by a bromine atom to the sulphur atom *via* the mercury atom (cf. **V**).

A similar effect (with Cl) may also involve **2** and **3a**. A measure of the above back-donation apparently also exists in the uncomplexed **1** and **2**; in these both the C_2–*S* and C_2–*N* bonds are shortened relative to tetrahydrothiophene and pyrrolidine (as mentioned). The effect is apparently maximal in **4** because of the back-donation from the bromine atom.

The C_2–N_3 and C_2–*S* distances in **4a** and **4b** (generally) show the usual inverse relationship *vis-à-vis* **1**, **2** and **3a**, as do the N_3–C_6 and C_6=*O* distances. The drastically lowered N_3–C_6 distance (1.2768 Å) in **4b** indicates the most enhanced level of amide resonance in this set of compounds; this is matched by the maximal *C*=*O* distance (1.2390 Å) observed in this set, but (intriguingly) not by the C_2–*S* length *vis-à-vis* **4a**.

Thus, the amide resonance is apparently not supported by the sulphur-to-nitrogen GAE. Intriguingly, the above maximal amide resonance (in **4b**) corresponds with electrophilic coordination at the sulphur atom! These trends possibly indicate a through-bond component to the sulphur-to-nitrogen GAE, which affects the S_1–C_2 and C_2–N_3 distances minimally, yet enhancing amide resonance.

3.6. The apparent immutability of the amide C=O bond

The amide carbonyl bond length apparently displays only marginal changes (except in **4b**). The changes in the *C*=*O* length are <0.016 Å, and generally an order of magnitude lower than those of the other lengths. In fact, an

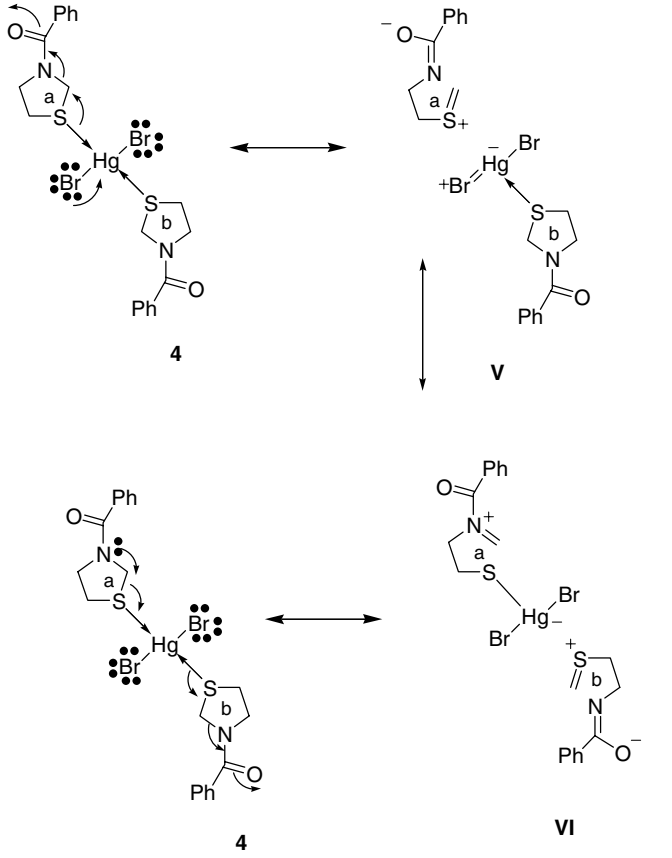

Scheme 5. The 'back-donation' mechanism in the $HgBr_2$ complex **4**, leading to an enhanced sulphur-to-nitrogen GAE *via* electron donation from the bromine atoms as shown in the no-bond form **V**. This is superimposed on the 'push–pull' mechanism depicted in **VI** (as in **3**, cf. Scheme 4). Thus, both the nitrogen-to-sulphur and sulphur-to-nitrogen GAE's operate in ring 'a', but only the latter in ring 'b' (these correspond to **4a** and **4b**, respectively in Tables 2, 5, 6, 8 and 9).

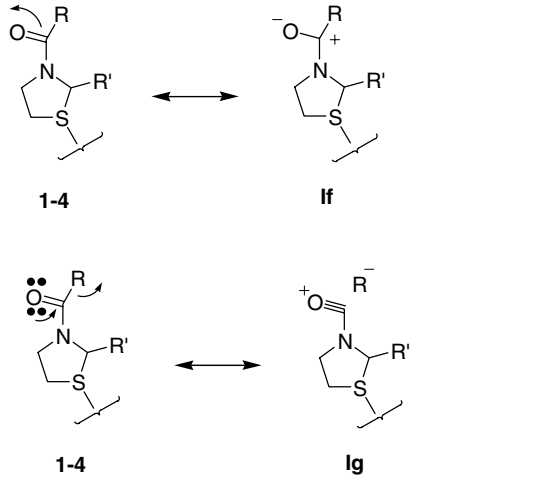

Scheme 6. The contribution of the canonical form **If** to the resonance of the amide group would be small if *R* were an electronegative group (as in **1** and **3**), but that of the no-bond form **Ig** would be considerable. (These explain the relative immutability of the *C*═*O* distance.)

inverse relationship with the neighbouring N_3–C_6 bond is to be expected on the basis of amide resonance (cf. canonical form **Ic**, Scheme 1); although this relationship exists in general, there are exceptions (*e.g.*, on going from **1** to **2** both *C*═*O* and N_3–C_6 increase).

A possible reason may be the contribution of the canonical form **If** (Scheme 6), which would be muted by an electron withdrawing group at C_6. This would explain the lower *C*═*O* length in **1** relative to **2** despite the shorter N_3–C_6 length in **1**, as also the nearly unchanged *C*═*O* length in **1** and its complex **3a.** An electron withdrawing substituent at C_6 could also raise the *C*═*O* bond order *via* overlap of an oxygen lone pair with the σ^* antibonding orbital at C_6 to the substituent (*cf.* canonical form **Ig**).

Therefore, the *C*═*O* bond is apparently subject to multiple (and compensatory) electronic effects, and so displays little change in geometry. However, the data in Table 2 is biased by the presence of the strongly electron withdrawing *p*-nitrophenyl group in two of the cases (**1** and **3**). Thus, considerable changes in the *C*═*O* length are observed in the other cases, those in the mercuric bromide complex **4** being clearly substantial.

3.7. Correlation with relevant spectroscopic characteristics

The salient features of the spectral data of **1**–**4** are collected in Table 4, and offer several interesting correlations with the crystallographic data (cf. Section 2 and Table 2).

The IR values for the amide *C*═*O* group correlate quite well with the N_3–C_6 bond lengths. The mercuric chloride complex **3** shows two IR bands for *C*═*O*, which accords with the fact that the two thiazolidine moieties are different: the band at 1650 cm^{-1} may be assigned to **3a** and the band at 1634 to **3b** on the basis of the 'push–pull' charge transfer discussed at length above (*cf.* Scheme 4).

However, the fact that the mercuric bromide complex **4** shows only one IR band for *C*═*O* is at odds with the *C*═*O* bond length data, which are far more different in **4a** and **4b** (relative to **3a** and **3b**). On the other hand, the very low value for the *C*═*O* IR band in **4** (1626 cm^{-1}) correlates very well with the drastically low N_3–C_6 length (1.2768 Å) and the maximal *C*═*O* length (1.2390 Å) observed in **4b.**

The above IR spectra were determined for the solids, so the crystal lattice was likely unperturbed. Also, the twin (*C*═*O*) bands in the IR spectrum of **3** are unlikely to be due to the rotational isomerism of the amide moiety, which was observed in solution (by NMR, *vide infra*) but not in the crystal (cf. Section 3.11). (The above ambiguity in the case of **4** remains unresolved.)

The NMR data also offer useful correlations, although the data is complicated by the rotational isomerism around the partial double bond (N_3–C_6) of the amide group. The shift values (both ^1H and ^{13}C) at C_2 of the thiazolidine ring indicate increasing positive charge in the series **1-5-3**, which accords both with the expected increase in the nitrogen-to-sulphur GAE and the S_1–C_2 lengths of **1** and **3** (Table 2). (The C_2 shift values of **2** and **4** are difficult to correlate with the others.)

The C_5–*H* resonances shift marginally upfield in **3** and **4** relative to **1** and **3**, respectively, although the ^{13}C resonance

Table 4
Salient spectroscopic characteristics of the *N*-acylthiazolidines **1**–**5** (cf. Sections 2.2 and 3.7)[a]

Thiazolidine derivative **1**–**5**	ν_{max} (cm^{-1}) (C=O)	δ_H (δ_C)			
		C_2	C_4	C_5	C_6 (δ_C)
N-(4-Nitrobenzoyl) (**1**)	1637 ($CHCl_3$)	4.47, 4.77 (50.7, 51.3)	3.75, 4.02 (48.0, 48.2)	3.05, 3.14 (29.5, 30.8)	166.8
N-Acetyl-2-phenyl (**2**)	1650 ($CHCl_3$)	6.01, 6.50 (64.0, 65.0)	3.95, 4.28 (50.2, 50.7)	3.04–3.17[b] (28.9, 30.4)	168.3, 169.1
$HgCl_2$ Complex (**3**)	1650, 1634 (KBr)	4.59, 4.72 (52.1, 52.2)	3.81, 3.93 (51.3, 51.4)	2.93, 3.12 (48.5, 49.2)	167.7
$HgBr_2$ Complex (**4**)	1626 (KBr)	4.64[b] (57.0, 57.5)	3.86[b] (51.3, 51.3)	2.91, 3.08 (45.7, 47.2)	169.8
N-Benzoyl (**5**)	1634 (KBr)	4.49, 4.73 (51.3)	3.75, 3.96 (48.0)	3.01[b] (30.4)	169.3

[a] Shown are the IR carbonyl stretching frequency of the *N*-acyl group (column 2), and the NMR chemical shifts (both ^1H and ^{13}C, the latter parenthesized) for the ring positions of the thiazolidine moiety (columns 3–5); the ^{13}C shift for the carbonyl carbon atom (C_6) is also given (column 6); the twin NMR resonances arise from rotational isomerism around the amide partial double bond.
[b] Broad.

shifts downfield in **3** relative to **1**. (Possibly, the ^{13}C shifts are more sensitive to through-bond charge transfer.) The ^{13}C NMR shifts of the amide carbonyl group (C_6) seem to vary erratically (rather like the *C=O* lengths discussed above). However, the observed downfield shift with an increase in the nitrogen-to-sulphur GAE (**1** *vs.* **3** and **4**), as also (possibly) with a decrease in amide resonance (**1** *vs.* **2** and **5**), are generally supported by the bond length data (Table 2).

3.8. Absence of pyramidalisation at N_3

An important question is whether the competition between amide resonance and the GAE in **1**–**4** leads to the pyramidalisation of the amidic N_3 centre [23]. (Pyramidalisation has been considered in the penicillins as a consequence of strain [24].)

There are three measures of pyramidalisation at an amide nitrogen centre [23,24]: the distance of the nitrogen atom from the plane formed by its three substituents ('*h* value'); the angle of deviation of the amide system from planarity (α); and the sum of the bond angles around the nitrogen atom (θ). The extent of pyramidalisation is proportional to *h*, α and the deviation of θ from 360°.

Of these α and θ are perhaps easier to employ. Their values in **1**–**4** are listed in Table 5. (The α has been estimated from the two torsion angles around the amide N_3–C_6 bond, involving the flanking endocyclic C_2 and C_4 atoms.) These show marginal, if any, pyramidalisation at N_3. Although θ is practically 360° in all the cases, α shows some variation, being as low as −161.6° in **3a**. This indicates some pyramidalisation, which interestingly correlates with an enhanced nitrogen-to-sulphur GAE in **3a**.

However, the general lack of pyramidalisation in **1**–**4** most likely implies that the nitrogen-to-sulphur GAE essentially involves the amide π system in its entirety. Apparently, this is energetically preferable to pyramidalising the amide nitrogen centre, so pyramidalisation is not a reliable measure of the perturbation of amide resonance.

Table 5
Possible pyramidalisation of the amide nitrogen atom (N_3) in **1**–**4**, as measured by the sum of the angles around N_3 (θ) and the torsion angle around the N_3–*CO* amide bond (α)[a]

Compound	θ (°)	α (°)[b]
1	359.3	0.79; 169.1
2	359.7	0.57; 174.0
3a	357.8	2.06; 161.6
3b	357.3	6.78; 169.0
4a	358.9	0.70; 167.0
4b	359.3	1.91; 167.9

[a] The values in parenthesis in the case of **3** and **4** refer to the second thiazolidine ring in the 2:1 complexes (cf. Schemes 2, 4 and 5).
[b] Signs omitted; the two values refer to the '*cisoid*' and '*transoid*' torsions (~0° and ~180°, respectively).

3.9. Ring puckering

The 1,3-thiazolidine ring in **1**–**4** is expectedly puckered (cf. Figs. 1–4 and Scheme 7). The ring torsion angles (cf. Table 6) indicate that the generally preferred conformation is the twisted envelope [25]: this is particularly so in the uncomplexed **1** and **2**, in which the C_5 atom occupies the 'flap' position as depicted in **Ih** (Scheme 7). The thiazolidine rings in the complexes **3** and **4** are less puckered, being nearly planar in **4**. The groups in the 'flap' position are different in **3a** and **3b**, as shown in **Ii** and **Ij**, respectively.

The envelope conformations of **1**–**3** are also supported by a Cremer and Pople analysis [26] of the crystallographic data, the magnitudes of $\varphi(2)$ (the phase angle) and $Q(T)$ (total puckering amplitude) being listed in Table 7. For an envelope conformation of a five membered ring, $\varphi(2)$ should be an integral multiple (k) of 36; [for a half-chair, $\varphi(2) = 36k + 18$]. The data in Table 7 indicates the

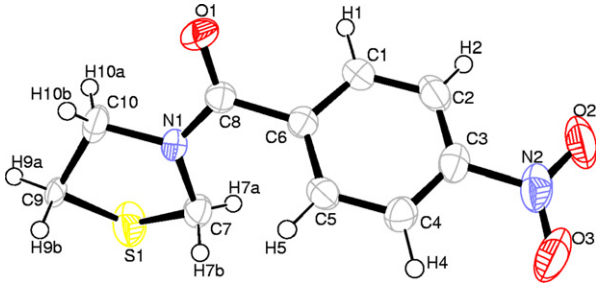

Fig. 1. ORTEP diagram of the asymmetric unit cell of the *N*-(4-nitrobenzoyl)-1,3-thiazolidine **1** at 50% ellipsoidal probability. (Crystallographic numbering is shown.)

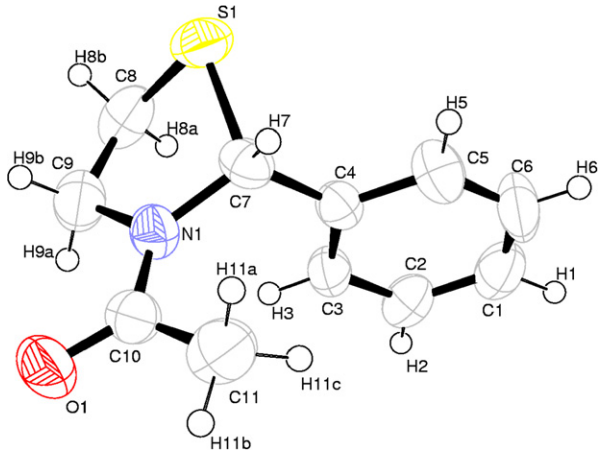

Fig. 2. ORTEP diagram of the asymmetric unit cell of the *N*-acetyl-2-phenyl-1,3-thiazolidine **2** at 50% ellipsoidal probability. (Crystallographic numbering is shown.)

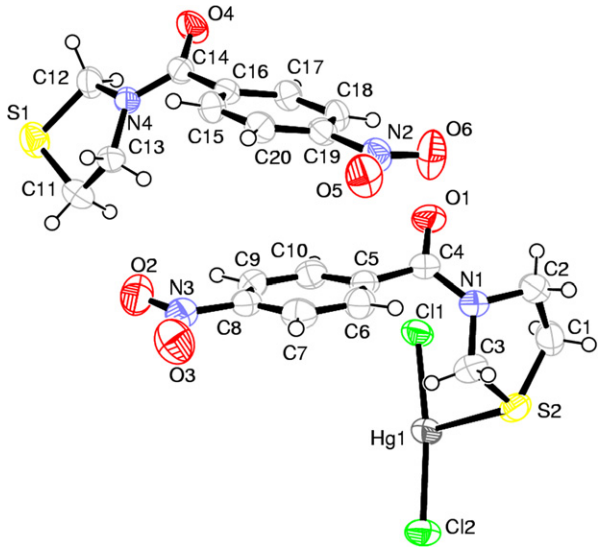

Fig. 3. ORTEP diagram of the asymmetric unit cell of the mercuric chloride complex **3** of *N*-(4-nitrobenzoyl)-1,3-thiazolidine at 50% ellipsoidal probability. (Crystallographic numbering is shown.)

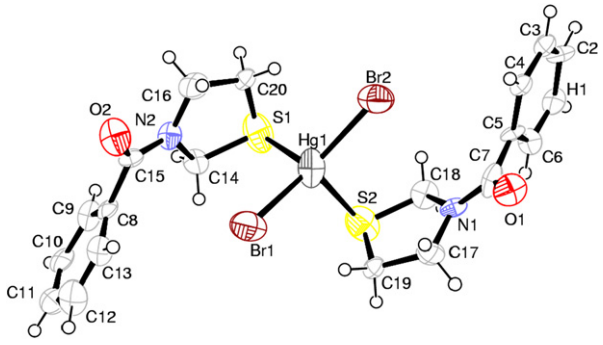

Fig. 4. ORTEP diagram of the asymmetric unit cell of the mercuric bromide complex **4** of *N*-benzoyl-1,3-thiazolidine at 50% ellipsoidal probability. (Crystallographic numbering is shown.)

envelope form for **1, 2, 3a** and **3b**, but not for **4a** and **4b**. (These computations were performed with the PLATON program developed by Spek [27].)

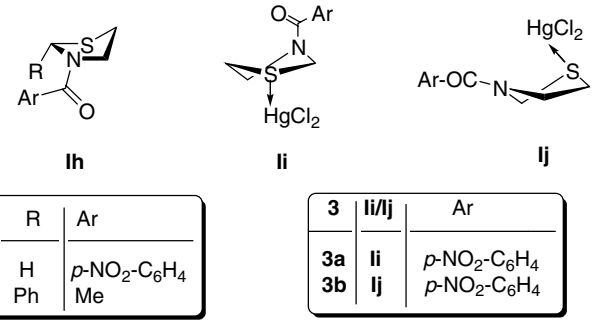

Ih	R	Ar
1	H	*p*-NO_2-C_6H_4
2	Ph	Me

3	Ii/Ij	Ar
3a	Ii	*p*-NO_2-C_6H_4
3b	Ij	*p*-NO_2-C_6H_4

Scheme 7. The observed ring puckerings are represented by the envelope form **Ih** and the twist forms **Ii** and **Ij**; the envelope **Ih** is apparently adopted by the uncomplexed **1** and **2**, whereas the twist forms **Ii** and **Ij** are preferred by the thiazolidine rings **3a** and **3b**, respectively in the $HgCl_2$ complex **3**. (The $HgBr_2$ complex **4** is nearly planar.)

Table 6
Puckering of the 1,3-thiazolidine ring in **1**–**4** as measured by the indicated torsion angles (in degree (°), cf. Scheme 7)[a]

Compound	S_1–C_2	N_3–C_2	N_3–C_4	C_5–C_4	S_1–C_5
1	−33.3(3)	15.1(3)	16.0(2)	−37.7(4)	40.6(4)
2	−34.7(3)	21.3(3)	7.2(1)	−33.3(4)	39.7(4)
3a	15.3(2)	−36.4(4)	44.0(1)	−29.6(3)	8.4(1)
3b	−21.0(3)	2.2(1)	22.5(2)	36.7(4)	33.7(4)
4a	−21.9(3)	17.7(3)	−5.4(1)	11.4(1)	19.4(1)
4b	−21.1(3)	18.5(3)	−8.4(1)	7.1(1)	16.0(2)

[a] These correspond to the following dihedral angles in the given order of atoms (sequentially in columns 2–6): C_5–S_1–C_2–N_3, C_4–N_3–C_2–S_1, C_2–N_3–C_4–C_5, S_1–C_5–C_4–N_3, C_2–S_1–C_5–C_4.

Table 7
Puckering in the thiazolidine rings in **1**–**4** in terms of the total puckering amplitude $Q(T)$, phase angle $\varphi(2)$ and k[a,b]

Compound	$Q(T)$ (Å)	$\varphi(2)$	k
1	0.5016 (6)	343.1 (7)°	10
2	0.4770 (2)	351.7 (5)	10
3a	0.3930 (4)	29.3 (5)	1
3b	03660 (4)	96.8 (5)	3
4a	0.2220 (3)	17.2 (3)	0.5
4b	0.2440 (2)	8.8 (5)	0.25

[a] Based on the method of Cremer and Pople, Refs. [26] and [27].
[b] $k = [\varphi(2)]/36$ should be an integer for an envelope conformation.

Previous reports had indicated the existence of various envelope and twist forms for the 1,3-thiazolidine ring, although with the nitrogen atom often in an out-of-plane position [6–8]. (This would bring the nitrogen lone pair of electrons into antiperiplanarity with the S_1–C_2 bond.) In **1**–**4** the nitrogen lone pair is part of an amide π system, and the nitrogen centre is not tetrahedral but (essentially) trigonal, so antiperiplanarity (with S_1–C_2) cannot be defined in the conventional sense. However, the general stereoelectronic requirement of overlap between the amide π system and the S_1–C_2 antibonding (σ^*) orbital (cf. Section 3.8), is fulfilled in various conformations including the planar (as indicated by models), although to varying extents.

The above π–σ^* overlap is most efficiently attained when the *N*–*C*–*S* system is planar, as in **Ih** (adopted by **1** and **2**, with

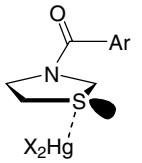

Ik

Ik	X	Torsion
3	Cl	~ 90°
4	Br	~ 70°

Scheme 8. The orientation of the mercury atom relative to the thiazolidine ligand in the mercury(II) complexes **3** and **4** is indicated in **Ik.** The N_3–C_2–*S-Hg* torsions of ~90° (in **3**) and ~70° (in **4**) suggest sp^2 hybridization at the sulphur. Coordination to the mercury atom occurs *via* a p-type orbital on sulphur (not shown), the free lone pair in an sp^2-like orbital more or less in the plane of the thiazolidine ring (shown in black) enabling the sulphur-to-nitrogen GAE in the planar ring.

C_5 at the 'flap'). In **Ii**, adopted by **3a**, N_3 occupies the 'flap', so the S_1–C_2 σ^* orbital is at an angle to the C_2–N_3–C_6 plane (comprising the amide π system); this accords with the (modest) pyramidalisation of N_3 observed in **3a** (cf. Section 3.8 above). In **Ij**, adopted by **3b**, S_1 occupies the 'flap', and again the S_1–C_2 σ^* orbital is at an angle to the C_2–N_3–C_6 plane, although this meets the stereoelectronic requirement for the sulphur-to-nitrogen GAE (*vide infra*).

The two thiazolidine moieties of the $HgBr_2$ complex **4** are puckered rather similarly, and indicate a nearly planar ring geometry, possibly because the sulphur-to-nitrogen GAE dominates in them. The N_3–C_2–*S–Hg* moiety subtends a dihedral angle of ~70° in both **4a** and **4b** (cf. **Ik**, Scheme 8). This indicates that the hybridization at the sulphur atom is somewhat close to sp^2, with the coordinating mercury atom bonding with a lone pair in the p orbital. This would leave the other free lone pair in an sp^2 orbital and more or less in the plane of the ring, and thus antiperiplanar to the C_2–N_3 bond: this would meet the stereoelectronic requirements for the sulphur-to-nitrogen GAE.

In **3** too, the N_3–C_2–*S–Hg* torsion is similar at ~90°, thus again indicating sp^2-like hybridization at the sulphur atom (cf. Scheme 8). Thus, this seems to be the general mode of operation of the sulphur-to-nitrogen GAE in the complexes **3** and **4**.

3.10. Bond angles and distances at S, N_3 and Hg

The annular bond angles at the sulphur atom are ~90° (cf. Table 8), similar to tetrahydrothiophenes (~95°) [15]. The marginally larger values in **4** are possibly due to the ~ sp^2 hybridization at the sulphur (*vide supra.*) The large annular bond angle at N_3 (~ 115°) relative to *N*-acylpyrrolidines (95°) [16] and other thiazolidines (106.5°) [8], is likely due to partial result of sp^2 hybridisation at N_3.

Table 8
Annular bond angles at the ring sulphur (S_1) and nitrogen (N_3) atoms in the 1,3-thiazolidine derivatives **1**–**4**

Compound	Angle at S_1 (°)	Angle at N_3 (°)
1	91.3(1)	114.5(2)
2	89.5(2)	115.5(2)
3a	92.8(1)	111.0(3)
3b	92.0(1)	115.5(4)
4a	98.2(3)	115.2(3)
4b	100.3(3)	113.4(2)

The bond angles at the mercury atoms are compatible with a trigonal bipyramidal (TBP) geometry (**VII**) [28] in **3** and a tetrahedral geometry (**VIII**) [28] in **4** (Table 9, Scheme 9). This is because **3** is dimeric and pentacoordinated at mercury, whereas **4** is monomeric and tetracoordinated at mercury. Thus, the dimeric **3** is comprised of two TBP moieties linked *via* a nearly rectangular $(HgCl)_2$ unit. (Apparently, Hg(II) prefers octahedral coordination, although other geometries are also known [28].)

The *Cl–Hg-Cl* angles of 83° and 173° in **3** indicate an approximate TBP structure, whereas the smaller *Br–Hg–Br* angle in **4** (~125°) indicates an approximate tetrahedral one (Table 9). In **3** (**VII**) the apices are occupied by two chlorine atoms ('Cl_{ap}') and the equatorial positions by two sulphur ('S_{eq}') and one chlorine ('Cl_{eq}') atom. The *S–Hg–S* angles in **3** (99°) and **4** (84°) are compatible with these assignments.

The tetrahedral (rather than square planar) geometry in **4** is indicated by the closely similar bond angles (108° and 113°) involving a given bromine atom and the two sulphur atoms (or *vice versa, cf.* Table 9). However, the widely differing *Br–Hg–Br* and *S–Hg–S* angles (125° and 84°, respectively) indicate a distorted tetrahedron at the mercury.

3.11. Orientation of the amide carbonyl group

The C_6=*O* group of the amide moiety is almost always oriented antiperiplanar to the C_2–N_3 bond (**Il**, Scheme 10). Thus, the C_2–N_3–C_6=*O* dihedral angle is ~180° (Table 10), indicating overlap between the antibonding σ^* orbital of the C_6–*O* σ bond and the electron density of the C_2–N_3 bond (strictly the 'HOMO'). (A similar effect, involving an alkyl-oxygen lone pair, exists in esters and lactones [1].) The lone exception is the case of **3b** in which the sulphur-to-nitrogen GAE dominates: thus, the C_2–N_3 bond would be partly broken so the above stereoelectronic overlap would be weak (the charge at N_3 being delocalized by amide resonance).

The above trends in the crystalline lattice, however, are at variance with the results of the solution state studies by NMR, which indicate that rotation around the amide N_3–C_6 bond is rapid at room temperatures (cf. Sections 2.4 and 3.7).

3.12. Possible relevance to the mechanism of action of penicillin

The key step in the mechanism of action of the penicillins (and the β-lactam antibiotics, in general) involves the cleavage of the β-lactam ring, *via* nucleophilic attack at its carbonyl group by a serine hydroxyl group of a bacterial transpeptidase enzyme [5,29] (cf. **IX**, Scheme 11). This also effectively (and irreversibly) inactivates the enzyme which is critically required for the construction of the bacterial cell wall, thereby destroying the bacterium itself. Although this

Table 9
Relevant bond angles at the mercury atom in the thiazolidine-HgX_2 complexes **3** and **4** (typical values only, cf. Scheme 9)

Compound	'X'	Angle X–Hg–X (°)	Angle S–Hg–S (°)	Angles X–Hg–S (°)
3	Cl	172.7(4),[a] 82.9(3)[b]	98.7(3)[c]	91.9(3)[b] 93.1(3)[b] 97.2(1)[c]
4	Br	124.4(9)	83.9(2)	107.9(2), 112.6(2)

[a] Apical–apical.
[b] Apical–Equatorial.
[c] Equatorial–Equatorial.

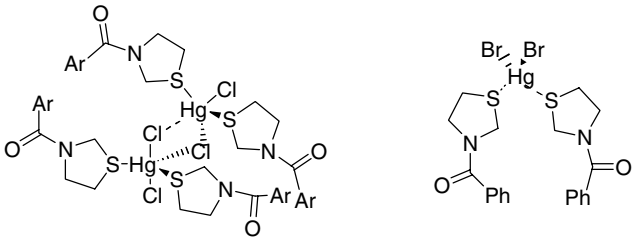

Scheme 9. The geometries at the mercury atom in the mercury(II) complexes **3** and **4:** the dimeric **3** adopts an approximate trigonal bipyramidal geometry as shown in **VII**, the central $(HgCl)_2$ unit – the site of dimerisation – forming a rectangle; however, the monomeric **4** adopts an approximate tetrahedral geometry as shown in **VIII**.

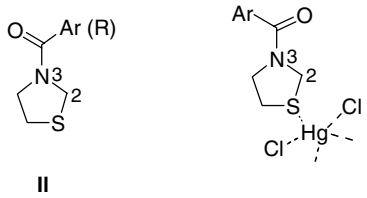

Scheme 10. The orientation of the N_3-acyl group in **1**–**4** is nearly always as shown in **II**, (C=O antiperiplanar to C_2–N_3), except in **3b** in which they are nearly synperiplanar, as shown in **Im**.

Table 10
The orientation of the N_3-acyl group in **1**–**4** as indicated by the C_2–N_3–C_6=O dihedral angle (cf. Scheme 10)

Compound	C_2–N_3–C_6=O torsion (°)
1	169.1(9)
2	174.0(8)
3a	−161.6(5)
3b	6.8(2)
4a	167.0(7)
4b	167.9(8)

indicates that the activity of the β-lactam antibiotics is related to their susceptibility to nucleophilic cleavage, it is noteworthy that they are stable to oral ingestion and pass through the digestive tract relatively unscathed. Thus, they possess a kinetic stability that is apparently lost at the transpeptidase active site, the basis of which has not been clarified.

An interesting possibility – that motivated this study and is apparently supported by it – is the diminution of the β-lactam amide resonance *via* an enhanced nitrogen-to-sulphur GAE at the active site [30,31]. The above results indicate that the *N*–*C*–*S* moiety in 1,3-thiazolidine is highly

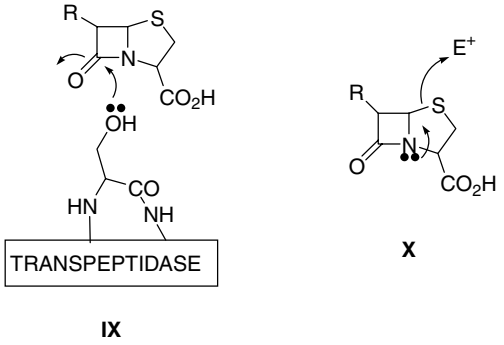

Scheme 11. Nucleophilic attack at the β-lactam carbonyl group in a penicillin by a serine hydroxyl group on a bacterial transpeptidase enzyme (**IX**), leading to the cleavage of the lactam and the irreversible inactivation of the enzyme (not shown). The possible activation of the β-lactam carbonyl group to nucleophilic attack (as in **IX**), *via* electrophilic coordination at the sulphur atom and an enhanced nitrogen-to-sulphur GAE is depicted in **X**. (E^+ represents the electrophile, which may be a proton, Zn(II), etc., in the enzymic case).

polarisable, and that electrophilic coordination at the sulphur atom can enhance the nitrogen-to-sulphur GAE (cf. **X**, Scheme 11).

It would be surprising if this possible mode of activation of the β-lactam antibiotics were not employed at the relevant enzyme active site. Although the toxicity of mercury(II) rules out its possible involvement as an electrophilic activator, two plausible alternatives may be mentioned: these are hydrogen bonding and zinc(II), the latter being a more reactive – and biocompatible – congener of Hg(II) in Group II B of the periodic table. Although further work may throw light on these possibilities, it is noteworthy that zinc(II) has indeed been implicated in the action of a class of β-lactamases (analogs of the transpeptidases in terms of their reactivity towards β-lactams) [32].

4. Conclusions

Crystal structures of the four *N*-acyl-1,3-thiazolidine derivatives **1**–**4** indicate that both the nitrogen-to-sulphur and the sulphur-to-nitrogen GAE's operate in them, although the former appears to dominate. Electrophilic coordination by mercury(II) at the sulphur atom apparently enhances the nitrogen-to-sulphur GAE in general. These effects are masked in some cases by other modes of charge transfer. An enhanced nitrogen-to-sulphur GAE diminishes the amide resonance of the *N*-acyl group. It seems pos-

sible that such an effect would form an important part of the mode of action of the β-lactam antibiotics.

Acknowledgements

We thank CSIR (New Delhi) and DST (New Delhi) for generous financial support of this work, including the CCD facility (DST) in the Division of Chemical Sciences, IISc. We thank Dr. Jyoti R. Kavali for preliminary investigations, and the referees for critical comments and helpful suggestions.

Appendix A

This section contains a brief note on the lattice packing in **1**–**4**, important crystallographic data obtained in this study in tabulated form (Tables A.1 and A.2), and plots of the relevant bond length data in Table 2 (Figs. 5–8, mentioned in Section 3.1.).

A note on the lattice packing in crystalline 1–4

There appears to be no uniform pattern to the lattice packing in the above thiazolidine derivatives [14].

Table A.1

Crystal data	*N*-(4-Nitrobenzoyl): **1**	*N*-Benzoyl-2-phenyl: **2**
Formula	$C_{10}H_{10}N_2O_3S_1$	$C_{11}H_{13}N_1O_1S_1$
CCDC No.	225,046	227,436
Temperature (K)	290(2)	290(2)
Radiation	Mo K_α	Mo K_α
Wavelength (Å)	0.7107	0.7107
Crystal system	Monoclinic	Orthorhombic
Space group	$P2_1/n$	$P2_12_12_1$
a (Å)	12.721(8)	9.295(6)
b (Å)	5.937(4)	9.482(6)
c (Å)	14.810(9)	11.842(7)
α (°)	90.00	90.00
β (°)	110.42(1)	90.00
γ (°)	90.00	90.00
Volume (Å^3)	1048.32(43)	1043.72(11)
Z	4	4
Density (g/cc)	1.51	1.32
Abs. Coeff. (mm^{-1})	0.301	0.275
$F(000)$	495.9	439.9
$\theta_{min,max}$	1.8, 25.3	2.8, 26.4
$h_{min,max}$, $k_{min,max}$, $l_{min,max}$	(−15, 13), (−7, 7), (−17, 17)	(−11, 11), (−11, 11), (−14, 14)
Number of reflections	7229	8177
Number unique reflections	1910	2101
Number of parameters	177	179
Refinement method	Full matrix leastsquares on F^2	Full matrix leastsquares on F^2
R_all	0.139	0.042.0.
R_obs	0.107	0.037
wR_2_all	0.263	0.081
wR_2_obs	0.247	0.079
$\Delta\rho_{min,max}$ (e Å^{-3})	−0.401, 0.489	−0.222, 0.144
Goodness-of-fit	1.236	1.12

Table A.2

Crystal data	$HgCl_2$ complex: **3**	$HgBr_2$ complex: **4**
Formula	$C_{20}H_{20}Cl_2Hg_1N_4O_6S_2$	$C_{20}H_{22}Br_2Hg_1N_2O_1S_2$
CCDC No.	225047	225048
Formula weight	748.0	746.9
Temperature (K)	293(2)	293(2)
Radiation	Mo K_α	Mo K_α
Wavelength (Å)	0.7107	0.7107
Crystal system	Triclinic	Triclinic
Space group	$P-1$	$P-1$
a (Å)	6.540(3)	5.907(9)
b (Å)	13.466(6)	12.597(20)
c (Å)	14.210(7)	15.426(26)
α (°)	80.35(1)	101.76(1)
β (°)	83.19(1)	100.64(3)
γ (°)	88.65(1)	90.18(6)
Volume (Å^3)	1225.06(21)	1113.40(43)
Z	2	2
Density (g/cc)	2.03	2.25
Abs. Coeff. (mm^{-1})	6.716	10.805
$F(000)$	723.8	707.8
$\theta_{min,max}$	1.5,26.4	1.6,24.7
$h_{min,max}$, $k_{min,max}$, $l_{min,max}$	(−8, 8), (−16, 16), (−17, 17)	(−6, 6), (−14, 13), (−18, 18)
Number of reflections	9503	5164
Number unique reflections	4787	2582
Number of parameters	396	262
Refinement method	Full matrix least squares on F^2	Full matrix least squares on F^2
R_all	0.028	0.099
R_obs	0.024	0.090
wR_2_all	0.063	0.231
wR_2_obs	0.061	0.221
$\Delta\rho_{min,max}$ (e Å^{-3})	−0.626, 0.857	−3.010, 2.703
Goodness-of-fit	1.03	1.055

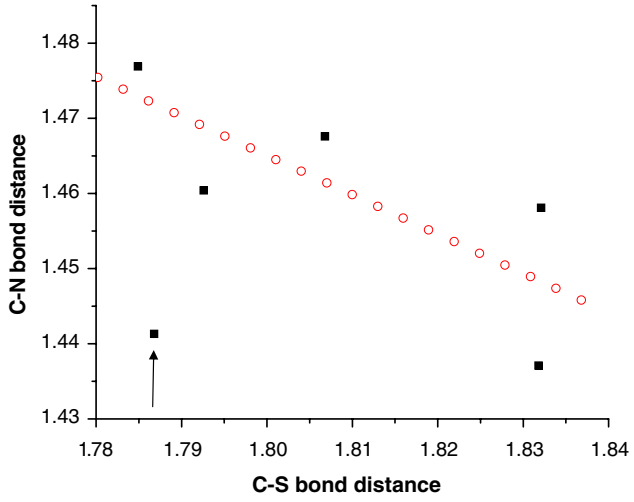

Fig. 5. A plot of the S_1–C_2 distance (x-axis) *vs.* the C_2–N_3 distance (y-axis) in **1**–**4** (cf. Table 2). The straight line (coloured circles) excludes the point indicated by the arrow (representing **4a**, in which both modes of the GAE are unusually enhanced). (The straight line obeys the equation: $y = 2.406 - 0.523x$, with correlation coefficient 'R' = 0.772.)

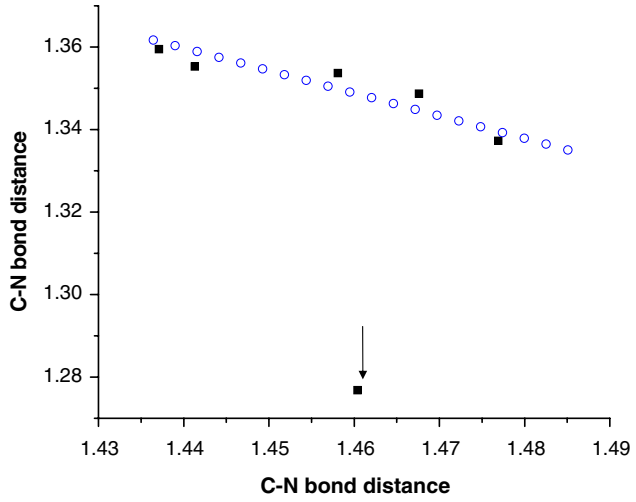

Fig. 6. A plot of the $C_2 - N_3$ distance (x-axis) *vs.* the N_3–C_6 distance (y-axis) in **1**–**4** (cf. Table 2). The straight line (coloured circles) excludes the point indicated by the arrow (representing **4b**). (The straight line obeys the equation: $y = 3.922 - 1.825x$, with correlation coefficient 'R' = 0.919.)

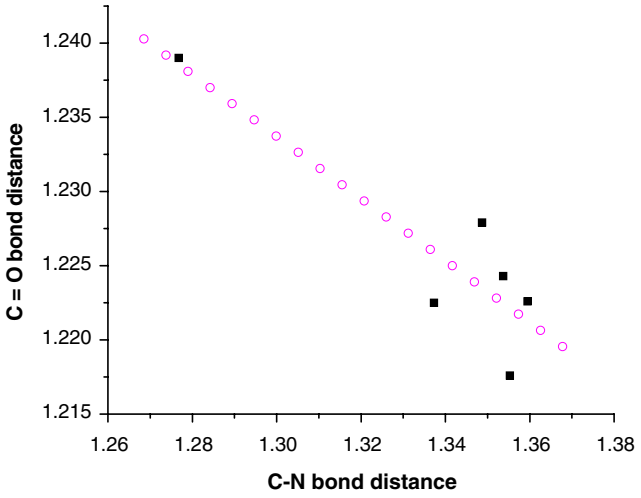

Fig. 7. A plot of the N_3–C_6 distance (x-axis) *vs.* the C_6=O distance (y-axis) in **1**–**4** (cf. Table 2). The straight line (coloured circles) includes all points and obeys the equation: $y = 1.505 - 0.209x$, with correlation coefficient 'R' = 0.888.

Although stacking and hydrogen bonding interactions determine the lattice packing, these are different in each case.

Thus, the parent 4-nitrobenzoyl derivative **1** exhibits stacking between the aromatic ring and the nitro group (involving both the nitrogen and oxygen atoms). The parent *N*-acetyl-2-phenyl derivative **2** shows hydrogen bonding interactions involving the aromatic π system and an aromatic *C*–*H* moiety. However, in the mercuric chloride complex **3**, π–π stacking involving the nitrophenyl rings are apparent in the asymmetric unit. Similar π–π stacking involving the phenyl rings of the *N*-benzoyl moiety are apparent in the mercuric bromide complex **4**, apart from hydrogen bonding interactions between the aromatic π system and an aromatic *C*–*H* moiety. (Thus, interestingly, the

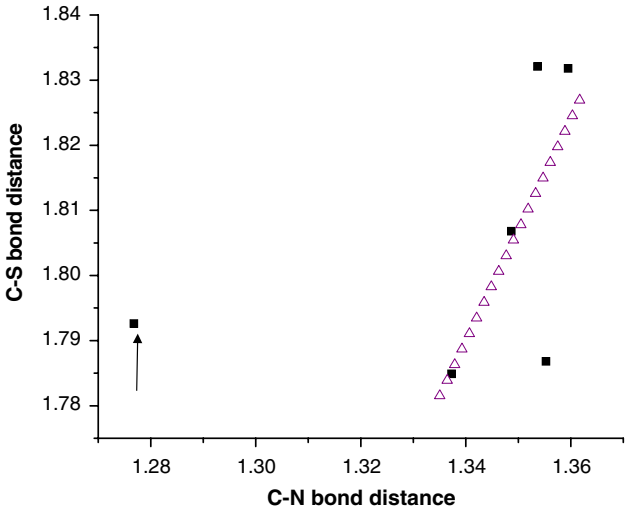

Fig. 8. A plot of the N_3–C_6 distance (x-axis) vs. the S_1–C_2 distance (y-axis) in **1**–**4** (cf. Table 2). The straight line (coloured triangles) excludes the point indicated by the arrow (representing **4b**). (The straight line obeys the equation: $y = -0.493 + 1.704x$, with correlation coefficient 'R' = 0.630.)

relatively lower amide resonance in the case of the complexes **3** and **4** seems to induce π–π stacking.)

All the derivatives **1**–**4** also display numerous (weak) hydrogen bonds involving *C*–*H* moieties in both the aromatic and thiazolidine rings as the usual donor, and an oxygen atom of the amide carbonyl or nitro group (when this is present) as the acceptor. In the case of **2** a hydrogen atom α to the carbonyl atom functions as a donor to several acceptors, including the thiazolidine sulphur atom. In the case of the complexes **3** and **4** hydrogen bonds involving the halogen atoms as the acceptors are also evident. These relatively weak (but numerous) interactions appear to contribute considerably to the lattice packing in all the above cases.

References

[1] A.J. Kirby, The Anomeric and Related Stereoelectronic Effects at Oxygen, Springer Verlag, Berlin, 1983.
[2] E. Juaristi, G. Cuevas, Tetrahedron 48 (1992) 5019.
[3] S. Chandrasekhar, Arkivoc xiii (2005) 37.
[4] J.V. Metzger, in: A.R. Katritzky, C.W. Rees, K.T. Potts (Eds.), Comprehensive Heterocyclic Chemistry, vol. 6, Pergamon Press, Oxford, 1984, p. 273, and references cited therein.
[5] G. Lowe, in: Sir Derek Barton, W.D. Ollis, E. Haslam (Eds.), Comprehensive Organic Chemistry, vol. 5, Pergamon Press, Oxford, Vol. 5, 1979, p. 289.
[6] R.C. Cambie, G.R. Clark, T.C. Jones, P.S. Rutledge, G.A. Strange, P.D. Woodgate, Aust. J. Chem. 38 (1985) 745.
[7] H.E. Howard-Lock, C.J.L. Lock, P.S. Smalley, Can. J. Chem. 63 (1985) 2411.
[8] F. Baert, M. Muller, D. Barbry, D. Couturier, Acta Crystallogr. B43 (1987) 538.
[9] E.L. Eliel, S.H. Wilen, L.N. Mander, Stereochemistry of Organic Compounds, Wiley, New York, 1994, p. 550.
[10] G.W. Stacy, P.L. Strong, J. Heterocycl. Chem. 5 (1968) 101.
[11] I.R. Schmolka, P.E. Spoerri, J. Am. Chem. Soc. 79 (1957) 4716.
[12] B.S. Furniss, A.J. Hannaford, V. Rogers, P.W.G. Smith, A.R. Tatchell, Vogel's Textbook of Practical Organic Chemistry, fourth ed., Longmans Group, Harlow, 1978, p. 683.

[13] N.A. Bell, T.N. Branston, W. Clegg, L. Parker, E.S. Raper, C. Sammon, C.P. Constable, Inorg. Chim. Acta 319 (2001) 130.
[14] Full details of our study have been deposited with the Cambridge Crystallographic Data Centre, 12 Union Road, Cambridge CB2 1EZ, U.K., (e-mail: deposit@ccdc.cam.ac.uk), and can be obtained by quoting the following depository numbers (sequentially for **1**–**4**): CCDC 225046, CCDC 227436, CCDC 225047, CCDC 225048.
[15] R.T. LaLonde, L. Codacovi, H. Cun-heng, X. Cang-fu, J. Clardy, B.S. Krishnan, J. Org. Chem. 51 (1986) 4899.
[16] M.G.B. Drew, A.V. George, N.S. Isaacs, H.S. Rzepa, J. Chem. Soc. Perkin Trans. 1 (1985) 1277.
[17] J. March, Advanced Organic Chemistry, fourth ed., Wiley, New York, 1992, p. 24, and references cited therein.
[18] B.M. Pinto, R.Y.N. Leung, in: G.R.J. Thatcher (Ed.), The Anomeric Effect and Associated Stereoelectronic Effects, ACS Symposium Series, vol. 539, American Chemical Society, Washington, DC, 1993, p. 146.
[19] J.M. Sprague, A.H. Land, in: R.C. Elderfield (Ed.), Heterocyclic Compounds, vol. 5, Wiley, New York, 1957, pp. 700–702.
[20] J. March, Advanced Organic Chemistry, fourth ed., Wiley, New York, 1992, p. 212 and references cited therein.
[21] J. Buckingham (Ed.), Dictionary of Organic Compounds, fifth ed., vol. 5, Chapman and Hall, New York, 1982, p. 5326.
[22] C.I. Braenden, Arkiv. Kemi. 22 (1964) 495.
[23] T. Ohwada, T. Achiwa, I. Okamoto, K. Shudo, Tetrahedron Lett. 39 (1998) 865.
[24] M.I. Page, Adv. Phys. Org. Chem. 23 (1987) 165.
[25] E.L. Eliel, S.H. Wilen, L.N. Mander, Stereochemistry of Organic Compounds, Wiley, New York, 1994, p. 758.
[26] D. Cremer, J.A. Pople, J. Am. Chem. Soc. 97 (1975) 1354–1358.
[27] A.L. Spek, Acta Crystallogr. Sect A 46 (1990) C34.
[28] N.N. Greenwood, A. Earnshaw, Chemistry of the Elements, second ed., Elsevier, Amsterdam, 1997, pp. 914, 1217.
[29] S. Coulton, I. François, Prog. Med. Chem. 31 (1994) 297.
[30] (a) S. Chandrasekhar, S. Srinivasa Gopalan, J. Chem. Res. (M) (2002) 1139;
(b) J. Chem. Res. (S) (2002) 532.
[31] K. Gopalaiah, Ph.D. Thesis, Indian Institute of Science, May 2005.
[32] M.S. Wilke, A.L. Lovering, N.C.J. Strynadka, Curr. Opin. Microbiol. 8 (2005) 525.